THE JOURNAL OF PHYSICAL CHEMISTRY A

Article

Cite This: J. Phys. Chem. A 2019, 123, 3344−3354

pubs.acs.org/JPCA

Three-Dimensional Reference Interaction Site Model Self-Consistent Field Study on the Coordination Structure and Excitation Spectra of Cu(II)−Water Complexes in Aqueous Solution

Chen Yang, Yoshihiro Watanabe, Norio Yoshida,* and Haruyuki Nakano*

Department of Chemistry, Graduate School of Science, Kyushu University, 744 Motooka, Nishi-ku, Fukuoka 819-0395, Japan

Supporting Information

ABSTRACT: The molecular and solvation structures of the hydrated Cu^{2+} ions and their excitation spectra were investigated using the Kohn−Sham density functional theory (DFT) and the three-dimensional reference interaction site model (3D-RISM) self-consistent field method. Five stable geometrical structures were found to exist in aqueous solution: the distorted octahedral $[Cu(H_2O)_6]^{2+}$ in C_i and D_{2h} symmetries, the square pyramidal and trigonal bipyramidal $[Cu(H_2O)_5]^{2+}$, and the square planar $[Cu(H_2O)_4]^{2+}$. The distorted octahedral structure in the C_i symmetry is preferred in $[Cu(H_2O)_6]^{2+}$, and the square pyramidal and trigonal bipyramidal $[Cu(H_2O)_5]^{2+}$ show almost the same stability. Among these geometries, the six-coordinate complex $[Cu(H_2O)_6]^{2+}$ in the C_i symmetry had the lowest Helmholtz energy. $[Cu(H_2O)_6]^{2+}$ had a distorted octahedral structure, that is, two long axial bonds and four short equatorial bonds. The spatial and radial distribution function analyses for $[Cu(H_2O)_5]^{2+}$ and $[Cu(H_2O)_4]^{2+}$ showed that $[Cu(H_2O)_5]^{2+}$ and $[Cu(H_2O)_4]^{2+}$ had one and two solvent water molecules that constituted a distorted octahedron with ligand water distribution. The coordination numbers (CNs) derived from the distribution functions were 5.2−5.4 for $[Cu(H_2O)_5]^{2+}$ and 5.3 for $[Cu(H_2O)_4]^{2+}$. These results indicated that the Cu^{2+} ion in an aqueous solution had 5−6 coordination water molecules in the first hydration shell and some structures with different CNs may interchange in the solution. The excitation energies and electronic configurations of low-lying d−d excited states were calculated using the time-dependent DFT with the electric field generated by 3D-RISM. The orbital energies and electronic configurations were in a similar picture to those of the classical crystal field theory because of the highly symmetrical features of all structures. In $[Cu(H_2O)_6]^{2+}$, the degeneracies of orbitals were resolved, whereas in $[Cu(H_2O)_5]^{2+}$ and $[Cu(H_2O)_4]^{2+}$, weak and strong quasi-degeneracies remained. As a result, only the four-coordinate complex generated third and fourth excited states, whereas in other complexes, there were no obvious characters of degeneracies. The resulting excitation energies were in good agreement with the absorption spectra.

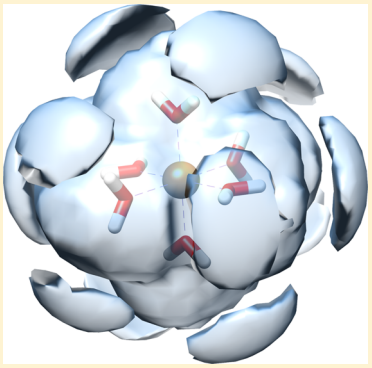

1. INTRODUCTION

Transition-metal ions show intrinsic optical absorption depending on the partially filled d-type orbital configurations. When the ions form complexes with ligands, their absorption spectra are also strongly affected by the configuration of coordinated ligands, that is, the number, geometry, and chemical nature of the ligands, and the absorption spectra shift by changing the configuration of ligands as a result of thermal fluctuations.

The shift in the optical absorption spectrum of transition-metal ions in aqueous solutions is one of the most fundamental issues. Among the transition metals, the Cu^{2+} ions, which ubiquitously exist in soil and biological systems, are of interest in a wide variety of fields, such as solution chemistry, biochemistry, and environmental chemistry; therefore, numerous experimental and computational studies have been conducted. However, even the number of coordinate water molecules and the geometries of hydrated complexes are still controversial.

According to the classical Jahn−Teller theorem, the Cu^{2+}−water complex is expected to take the sixfold octahedral structure. However, the combinatorial study of neutron diffraction and ab initio molecular dynamics (MD) simulations by Pasquarello et al. has broken the mold of this classical picture.[1] They argued that the five-coordinate structure is more favorable than the six-coordinate structure and the five-coordinate structure takes transformable configurations between square pyramidal and trigonal bipyramidal structures. Their results caused a lengthy debate. Their argument was contradicted by Persson et al. who supported the conventional sixfold structure based on low-angle X-ray spectroscopy and extended X-ray absorption fine structure (EXAFS) data.[2] To date, the intensive scrutiny of this model is continued by both experimental and computational studies.[3−10] This situation originates from the difficulties in distinguishing between the four-, five-, and six-coordinate structures of the Cu^{2+}−water complex because the energetic differences between them are very small.[6,7] Therefore, to know the optical properties of the

Received: February 12, 2019
Revised: March 21, 2019
Published: March 21, 2019

DOI: 10.1021/acs.jpca.9b01364
J. Phys. Chem. A 2019, 123, 3344−3354

Cu^{2+}−water complex, the possibility of taking multiple configurations of the complex, as well as the solvent water surrounding the complex, must be appropriately considered.

In the present paper, we examine the molecular, electronic, and solvation structures of $[Cu(H_2O)_n]^{2+}$ (n = 4−6) using the hybrid method of Kohn−Sham density functional theory (KS-DFT) and the three-dimensional reference interaction site model (3D-RISM) method, which we call KS-DFT/3D-RISM or 3D-RISM self-consistent field (3D-RISM-SCF) method.[11,12] The Cu^{2+} ion and the first contact n-water molecules were regarded as solute species and treated by quantum mechanics, whereas all other water molecules were regarded as classical solvents and treated by statistical mechanics. Thus, the 3D-RISM-SCF method provides both the electronic structure of the solute and the solvation structure. The aim of the present work was to elucidate the structure of the Cu^{2+}−water complex and the optical absorption spectrum in an aqueous solution. We considered a four-, five-, and six-coordinate hydrated Cu^{2+} complex immersed in aqueous solution. In a previous paper,[13] we applied the same method to the electronic structure of Cr^{3+} in an aqueous solution. We modeled Cr^{3+} ion and the first contact solvent water molecules as hexahydrated chromium trication $[Cr(H_2O)_6]^{3+}$ and obtained a detailed 3D distribution around $[Cr(H_2O)_6]^{3+}$, which showed 12 maximum density points arising from hydrogen bonds, as well as eight local maximum points at the hollow sites, in the second hydration shell. We also obtained the low-lying excited states of vertical transitions using a time-dependent DFT (TD-DFT) that included the electric field from the solvent produced by the 3D-RISM-SCF method. The computed excited energies agreed well with the available experimental values. These results indicated that the method employed here was suitable for investigating the configuration of the Cu^{2+}−water complex and its effects on optical absorption. One major difference from the Cr^{3+} case is that Cr^{3+} has a nondegenerate ground state, whereas Cu^{2+} with the d^9 electron configuration has a quasi-degenerate ground state. This quasi-degeneracy is probably an origin of the question on the coordination numbers (CNs). It gives the Cu^{2+}−water complex distorted geometries and makes the excitation spectra rather complicated. Clarifying these complicated molecular and electronic structures was also the aim of the present paper.

The organization of this paper is as follows. In Section 2, we describe the computational method and the details of the calculations used in the present paper. Section 3 shows the results of the calculations. The optimized structure of $[Cu(H_2O)_n]^{2+}$ (n = 4−6) complexes, the solvation structure, the ground- and excited-state electronic structures, and vertical excitation energies are also reported and discussed in Section 3. Conclusions are given in Section 4.

2. COMPUTATIONAL METHODS

2.1. Brief Overview of the 3D-RISM-SCF Method. The 3D-RISM-SCF method is a hybrid method of the electronic structure theory and the integral equation theory of liquids (3D-RISM theory).[11,12] In this method, solute molecules are treated by quantum chemistry and solvent molecules are treated by statistical mechanics; thereby, the electron density in the DFT (or the electronic wave function) of the solute molecule and the distribution of the solvent [spatial distribution function (SDF), $g_\gamma(\mathbf{r})$, where γ indicates the solvent site] around the solute are determined simultaneously.

The Helmholtz energy (A) of the solute−solvent system is defined as

$$A = E_{\text{solute}} + \Delta\mu \tag{1}$$

where E_{solute} is the solute electronic energy computed from the quantum chemical electronic structure theory and $\Delta\mu$ is the excess chemical potential from the solute−solvent interaction. The first term on the right-hand side (rhs) of eq 1, E_{solute}, is given by

$$E_{\text{solute}} = F_0[n_{\text{solv}}(\mathbf{r}_{\text{elec}})] \tag{2}$$

for DFT, where F_0 is the energy functional for the isolated solute molecule and $n_{\text{solv}}(\mathbf{r}_{\text{elec}})$ is the electron density of the solute molecules in the solution, and

$$E_{\text{solute}} = \langle \Psi_{\text{solv}} | \hat{H}_0 | \Psi_{\text{solv}} \rangle \tag{3}$$

for the wave function theory, where $\hat{H}_0$ is the Hamiltonian of the isolated solute molecule and Ψ_{solv} is the electronic wave function of the solute molecule in the solution. The second term of the rhs of eq 1, $\Delta\mu$, is given by

$$\Delta\mu = \rho_\nu \int_0^1 d\lambda \int d\mathbf{r} \sum_{\gamma \in \text{solvent}} u_\gamma(\mathbf{r}) g_\gamma^\lambda(\mathbf{r}) \tag{4}$$

where λ and $g_\gamma^\lambda(\mathbf{r})$ are an order parameter for thermodynamic integral and the 3D distribution function at state λ, respectively. $u_\gamma(\mathbf{r})$ denotes the 3D distribution function and the solute−solvent interaction potential, respectively. If we use the Kovalenko−Hirata (KH) closure[11,14]

$$h_\gamma(\mathbf{r}) = \begin{cases} \exp(d_\gamma(\mathbf{r})) - 1 & \text{for } d_\gamma(\mathbf{r}) \le 0 \\ d_\gamma(\mathbf{r}) & \text{for } d_\gamma(\mathbf{r}) > 0 \end{cases} \tag{5}$$

$$d_\gamma(\mathbf{r}) = -\frac{u_\gamma(\mathbf{r})}{k_B T} + h_\gamma(\mathbf{r}) - c_\gamma(\mathbf{r}) \tag{6}$$

the integration with respect to λ in eq 4 can be performed analytically and the equation becomes

$$\Delta\mu = \rho_\nu k_B T \sum_{\gamma \in \text{solvent}} \int d\mathbf{r} [(h_\gamma(\mathbf{r}))^2 \Theta(-h_\gamma(\mathbf{r}))/2 - c_\gamma(\mathbf{r}) - h_\gamma(\mathbf{r}) c_\gamma(\mathbf{r})/2] \tag{7}$$

where k_B and T indicate the Boltzmann constant and the absolute temperature, respectively, and ρ_ν is the number density of solvent species ν. The functions $h_\gamma(\mathbf{r}) = g_\gamma(\mathbf{r}) - 1$ and $c_\gamma(\mathbf{r})$ are the 3D total and direct correlation functions of the solvent site γ, respectively, and $\Theta(x)$ is the Heaviside step function. The solute−solvent interaction potential, $u_\gamma(\mathbf{r})$, is given by

$$u_\gamma(\mathbf{r}) = \sum_{\alpha \in \text{solute}} \left\{ 4\varepsilon_{\alpha\gamma} \left[\left(\frac{\sigma_{\alpha\gamma}}{|\mathbf{r} - \mathbf{r}_\alpha|} \right)^{12} - \left(\frac{\sigma_{\alpha\gamma}}{|\mathbf{r} - \mathbf{r}_\alpha|} \right)^{6} \right] + \int \frac{q_\gamma n_{\text{solv}}(\mathbf{r}_{\text{elec}})}{|\mathbf{r} - \mathbf{r}_{\text{elec}}|} d\mathbf{r}_{\text{elec}} \right\} \tag{8}$$

where $\varepsilon_{\alpha\gamma}$ and $\sigma_{\alpha\gamma}$ denote the Lennard-Jones (LJ) parameter between sites α and γ, respectively, with usual meanings, and q_γ is a point charge on the solvent site γ.

DOI: 10.1021/acs.jpca.9b01364
J. Phys. Chem. A 2019, 123, 3344−3354

Table 1. Ground-State Helmholtz Energies of $[Cu(H_2O)_{4-6}]^{2+}$ in Aqueous Solution (in a.u.)

structure	A	E_{solute} (E_{reorg} + E_{iso})	$\Delta\mu$
$[Cu(H_2O)_6]^{2+}$			
square bipyramidal (C_i)	−2098.2728	−2098.0567 (0.002−2098.0569)	−0.2161
square bipyramidal (D_{2h})	−2098.2632	−2098.0437 (0.001−2098.0438)	−0.2196
$[Cu(H_2O)_5]^{2+}$			
square pyramidal	−2021.8770	−2021.6380 (0.0007−2021.6387)	−0.2390
trigonal bipyramidal	−2021.8767	−2021.6421 (0.0002−2021.6423)	−0.2346
$[Cu(H_2O)_4]^{2+}$			
square planar	−1945.4882	−1945.2085 (0.0046−1945.2131)	−0.2797
H_2O[a]	−76.3782	−76.3670 (0.0062−76.3732)	−0.0111

[a]A water molecule in aqueous solution. The solute energy (E_{solute}) can decompose into solute reorganization energy (E_{reorg}) and total energy (E_{iso}) of the solute molecule in an isolated condition.

As can be seen from eqs 1−7, the Helmholtz energy is a functional of the electronic density n_{solv} (or the electronic wave function Ψ_{solv}) of the solute molecule and the correlation functions $h_\gamma(\mathbf{r})$ and $c_\gamma(\mathbf{r})$: $A = A[n_{solv}$ (or Ψ_{solv}), $h_\gamma(\mathbf{r})$, $c_\gamma(\mathbf{r})]$. The basic equations of the 3D-RISM-SCF method are derived by the variation of the Helmholtz energy with respect to n_{solv} (or Ψ_{solv}), $h_\gamma(\mathbf{r})$, and $c_\gamma(\mathbf{r})$. If we adopt the KS-DFT for the solute electronic structure theory, the resulting equation for the solute molecules is the KS equation for the KS operator $\hat{f}$ that includes the interaction from the solvent

$$\hat{f}\,\varphi(\mathbf{r}_{elec}) = \varepsilon\varphi(\mathbf{r}_{elec}) \tag{9}$$

where ε and $\varphi(\mathbf{r})$ are the orbital energy and KS orbital, respectively. The equation for the solvent is the 3D site Ornstein−Zernike equation

$$h_\gamma(\mathbf{r}) = c_{\gamma'}(\mathbf{r})*(\omega^{vv}_{\gamma'\gamma}(r) + \rho_v h^{vv}_{\gamma'\gamma}(r)) \tag{10}$$

supplemented by the KH closure relation, eq 5, where $\omega^{vv}_{\gamma\gamma'}(r)$ and $h^{vv}_{\gamma\gamma'}(r)$ are the site−site intramolecular and total correlation functions of the pure solvent system, respectively (superscript "v" denotes the solvent). The symbol * indicates convolution in direct space and summation over repeated site indices. These functions, $\omega^{vv}_{\gamma\gamma'}(r)$ and $h^{vv}_{\gamma\gamma'}(r)$, are computed beforehand by solving the one-dimensional RISM equation for a pure solvent system once before the 3D-RISM-SCF calculation.

2.2. Computational Details. The geometries of the ground-state electronic structures of $[Cu(H_2O)_n]^{2+}$ (n = 4−6) and the solvent distributions around the ions were determined by the 3D-RISM-SCF method. The excited states were obtained using TD-DFT. Gas-phase calculations were also performed for comparison with calculations for the solution phase. The electronic structure method for the solute molecules used in the 3D-RISM-SCF method was DFT with the PBE0 hybrid functional,[15,16] which consists of the Perdew−Burke−Ernzerhof (PBE) 1996 (0.75) + Hartree−Fock (0.25) exchange and PBE 1996 nonlocal (1.0) + Perdew−Wang 1991 LDA local (1.0) correlation functionals. The functional dependency was checked using other functionals and confirmed to be small. The basis set used was the correlation-consistent polarized valence triple-zeta (cc-pVTZ) set.[17,18]

The parameters used in the 3D-RISM-SCF method were as follows. The temperature and density of solvent water were 298 K and 0.03334 molecules per Å^3, respectively. Effective point charges were used to describe the solute−solvent interaction potential. The effective point charges on the solute molecule were determined to reproduce the electrostatic potential around the solute molecule by using least-square fitting. The LJ parameters (σ, ε) for Cu, H, and O were (2.2 Å, 0.0125 kcal/mol), (0.4 Å, 0.046 kcal/mol), and (3.166 Å, 0.1554 kcal/mol), respectively. The extended simple point charge model (SPC/E) parameter set for the geometrical and potential parameters for the solvent water was used with modified H parameters (σ = 0.4 Å and ε = 0.046 kcal/mol).[19] The grid points in the 3D-RISM calculations were 128 × 128 × 128 with a spacing of 0.25 Å.

All the calculations were performed with a modified version of the GAMESS program package,[20] where the 3D-RISM-SCF method and their gradient methods have been implemented.[21]

3. RESULTS AND DISCUSSION

The Helmholtz energies and geometries of $[Cu(H_2O)_n]^{2+}$ (n = 4−6) in an aqueous solution calculated with the 3D-RISM-SCF method are summarized in Tables 1−3. The geometries

Table 2. Relative Values from Helmholtz Energy of $[Cu(H_2O)_6]^{2+}$ in C_i Symmetry (in kcal/mol)

structure	ΔA	ΔE_{solute} (ΔE_{reorg} + ΔE_{iso})	$\Delta\Delta\mu$
$[Cu(H_2O)_6]^{2+}$			
square bipyramidal (C_i)	0.00	0.00 (0.00 + 0.00)	0.00
square bipyramidal (D_{2h})	6.05	8.15 (0.03 + 8.12)	−2.16
$[Cu(H_2O)_5]^{2+}$ + H_2O			
square pyramidal	11.09	32.42 (4.24 + 28.18)	−21.34
trigonal bipyramidal	11.24	29.87 (3.93 + 25.94)	−18.62
$[Cu(H_2O)_4]^{2+}$ + $2H_2O$			
square planar	17.74	71.63 (10.56 + 61.07)	−53.89

DOI: 10.1021/acs.jpca.9b01364
J. Phys. Chem. A 2019, 123, 3344−3354

Table 3. Cu−O Bond Distances and O−Cu−O Angles of $[Cu(H_2O)_{4-6}]^{2+}$ (in Å and deg)[a,b,c]

structure	r_{ax}		r_{eq}/O−Cu−O angle			
$[Cu(H_2O)_6]^{2+}$						
square bipyramidal (C_i)	2.28 (2.271)	2.28 (2.271)	2.00 (2.012)	1.97 (2.000)	2.00 (2.012)	1.97 (2.000)
			90.0 (90.0)	90.0 (90.0)	90.0 (90.0)	90.0 (90.0)
square bipyramidal (D_{2h})	2.25 (2.300)	2.25 (2.300)	2.04 (2.059)	1.96 (1.973)	2.04 (2.059)	1.96 (1.973)
			90.0 (90.0)	90.0 (90.0)	90.0 (90.0)	90.0 (90.0)
$[Cu(H_2O)_5]^{2+}$						
square pyramidal	2.10	–	1.98	1.97	1.97	1.95
			100.0	92.0	102.0	98.0
trigonal bipyramidal	1.93	1.93	2.06	2.04	2.03	
			91.0	90.0	90.0	
$[Cu(H_2O)_4]^{2+}$						
square planar	–	–	1.95 (1.956)	1.95 (1.956)	1.95 (1.954)	1.95 (1.954)

[a]The values in the parentheses are bond distances and angles in vacuum. [b]r_{ax} and r_{eq} denote the axial and equatorial bond length, respectively. [c]The precision of the bond distances and bond angles by the 3D-RISM-SCF method is two and zero decimal places, respectively, because of the grid size (0.25 Å) in the 3D-RISM calculations.

are illustrated in Figure 1. The solvent distributions (SDFs) for the optimized geometries obtained through the 3D-RISM-SCF

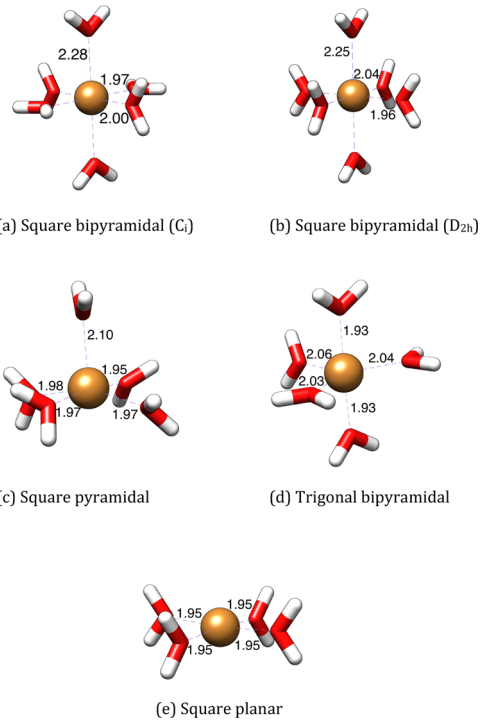

Figure 1. Optimized geometries of $[Cu(H_2O)_6]^{2+}$ (square bipyramidal structures in C_i (a) and D_{2h} (b) symmetries), $[Cu(H_2O)_5]^{2+}$ (square pyramidal (c) and trigonal bipyramidal (d) structures), and $[Cu(H_2O)_4]^{2+}$ (square planar structure (e)).

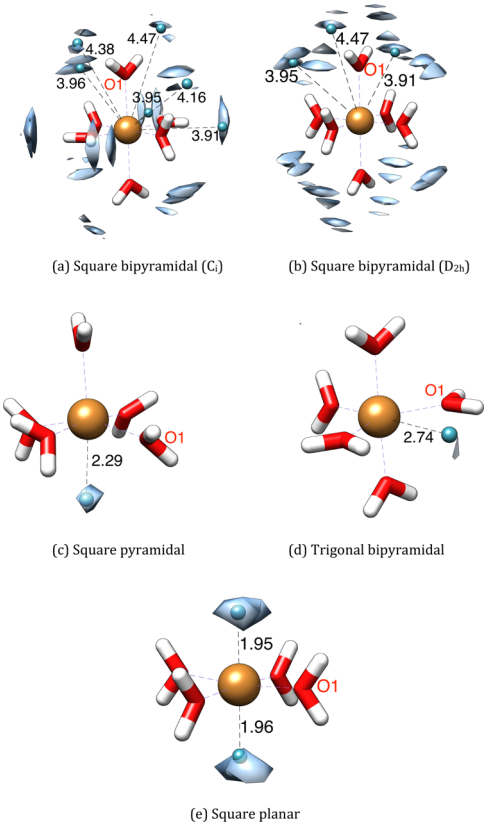

Figure 2. SDFs of O for $[Cu(H_2O)_6]^{2+}$ (square bipyramidal structures in C_i (a) and D_{2h} (b) symmetry), $[Cu(H_2O)_5]^{2+}$ (square pyramidal (c) and trigonal bipyramidal (d) structures), and $[Cu(H_2O)_4]^{2+}$ (square planar structure (e)).

method are shown in Figure 2a−e. In addition, the radial distribution functions (RDFs) of O and H from the Cu atom obtained by angular averaging of the SDFs as well as the CN of O are depicted in Figure 3a−j. The energies of the d-type KS orbitals at the optimized geometries in solution are listed in Table 4 and depicted in Figure 4. The excitation energies and characters of the d−d excited states in solution obtained by the TD-DFT method are summarized in Table 5 and Figure 5.

3.1. Overview of Energetics of Four-, Five-, and Six-Coordinate Complexes $[Cu(H_2O)_{4-6}]^{2+}$. First, we will discuss the energetics of the four-, five-, and six-coordinate complexes in an aqueous solution (molecular and solvation structures are discussed in detail in the following subsections). We optimized the structures of $[Cu(H_2O)_4]^{2+}$, $[Cu(H_2O)_5]^{2+}$, and $[Cu(H_2O)_6]^{2+}$ (and H_2O) in an aqueous solution using the 3D-RISM-SCF/PBE0 method. The initial structures for the optimization were square planar and tetrahedral structures for $[Cu(H_2O)_4]^{2+}$, square pyramidal and trigonal bipyramidal structures for $[Cu(H_2O)_5]^{2+}$, and an octahedral structure for $[Cu(H_2O)_6]^{2+}$, which were taken from the literature.[1,10] The tetrahedral structure of $[Cu(H_2O)_4]^{2+}$ was unstable and converged to the square planar structure. Both the square

DOI: 10.1021/acs.jpca.9b01364
J. Phys. Chem. A 2019, 123, 3344−3354

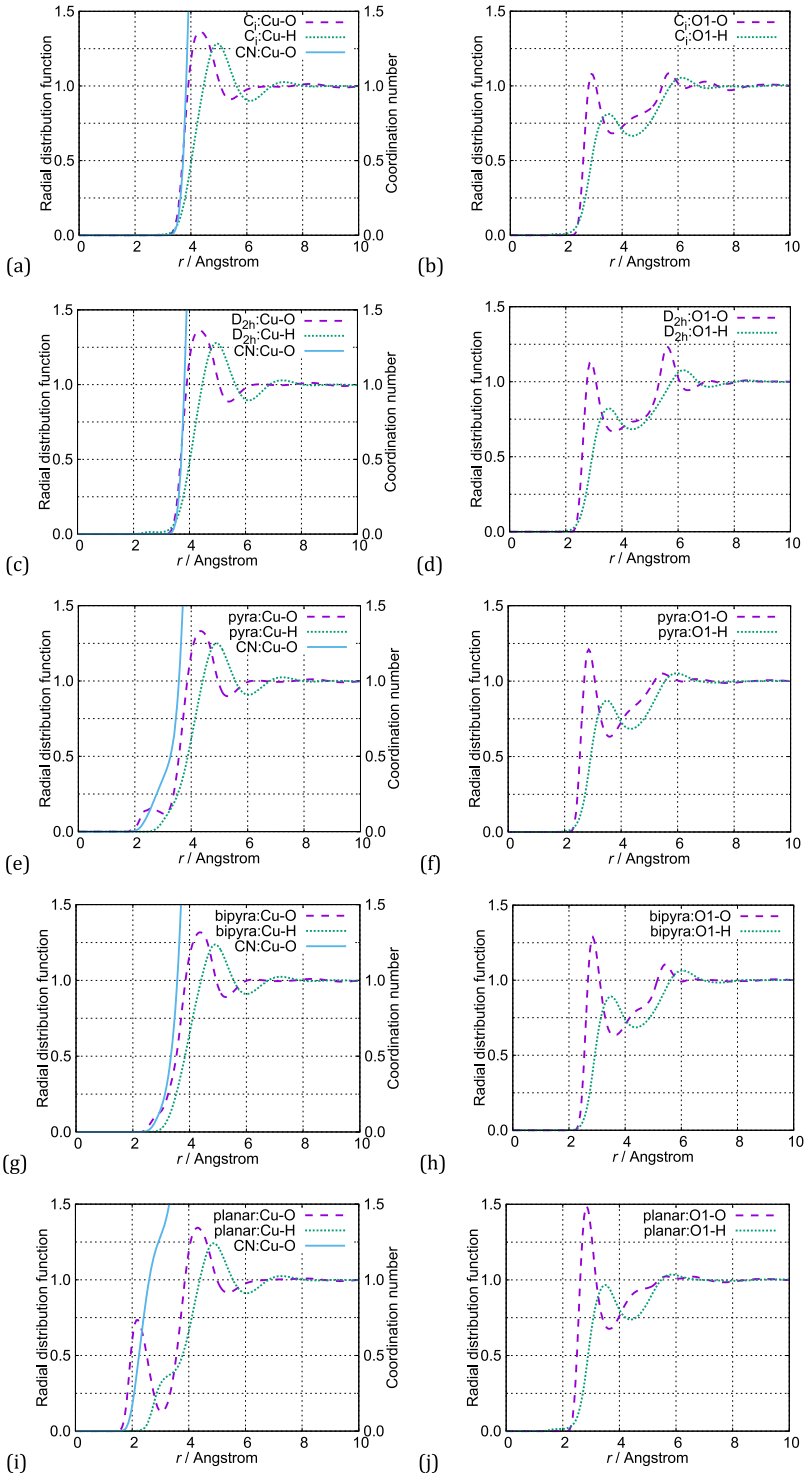

Figure 3. RDFs of O and H from Cu and CN of O from Cu for $[Cu(H_2O)_6]^{2+}$ (Square bipyramidal structures in C_i (a) and D_{2h} (c) symmetries), $[Cu(H_2O)_5]^{2+}$ (square pyramidal (e) and trigonal bipyramidal (g) structures), and $[Cu(H_2O)_4]^{2+}$ (square planar structure (i)). RDFs of O and H from the O atom marked in Figure 2 for $[Cu(H_2O)_6]^{2+}$ (square bipyramidal structures in C_i (b) and D_{2h} (d) symmetries), $[Cu(H_2O)_5]^{2+}$ (square pyramidal (f) and trigonal bipyramidal (h) structures), and $[Cu(H_2O)_4]^{2+}$ (square planar structure (j)).

pyramidal and trigonal bipyramidal structures of $[Cu(H_2O)_5]^{2+}$ were stable in an aqueous solution; however, they were unstable in vacuum. Two square bipyramidal (i.e., nearly octahedral) structures in C_i and D_{2h} symmetries were obtained for $[Cu(H_2O)_6]^{2+}$.

The Helmholtz energies at the optimized structures are summarized in Tables 1 and 2. In Table 2, the total energies of $[Cu(H_2O)_4]^{2+} + 2H_2O$ and $[Cu(H_2O)_5]^{2+} + H_2O$ are also listed, where two water molecules and one water molecule of the solvent were treated explicitly by quantum mechanics to enable direct comparison of different coordinate complexes. Among the optimized structures, $[Cu(H_2O)_6]^{2+}$ in the C_i symmetry had the lowest Helmholtz energy. $[Cu(H_2O)_6]^{2+}$ in the D_{2h} symmetry was 6.05 kcal/mol higher than the lowest.

DOI: 10.1021/acs.jpca.9b01364
J. Phys. Chem. A 2019, 123, 3344−3354

Table 4. Energies of d-Type Kohn−Sham Orbitals of $[Cu(H_2O)_{4-6}]^{2+}$ in Aqueous Solution (in eV)[a]

Structure	occ1	occ2	occ3	occ4	uoc1
$[Cu(H_2O)_6]^{2+}$					
square bipyramidal (C_i)	$d_{xy}(\pi)$	d_{xz}	$d_{yz}(\pi^*)$	$d_{z^2}(\sigma^*)$	$d_{x^2-y^2}(\sigma^*)$
	−13.34 (H − 9)	−12.12 (H − 7)	−10.98 (H − 3)	−10.38 (H)	−4.60 (L)
square bipyramidal (D_{2h})	d_{xz}	d_{yz}	$d_{xy}(\pi^*)$	$d_{z^2}(\sigma^*)$	$d_{x^2-y^2}(\sigma^*)$
	−12.41 (H − 8)	−11.97 (H − 7)	−11.33 (H − 4)	−10.47 (H)	−4.67 (L)
$[Cu(H_2O)_5]^{2+}$					
square pyramidal	$d_{yz}(\pi)$	$d_{xz}(\pi)$	$d_{xy}(\pi^*)$	$d_{z^2}(\sigma^*)$	$d_{x^2-y^2}(\sigma^*)$
	−12.94 (H − 7)	−12.61 (H − 6)	−11.85 (H − 5)	−10.96 (H)	−4.93 (L)
trigonal bipyramidal	$d_{xz}(\pi)$	$d_{yz}(\pi)$	$d_{x^2-y^2}(\sigma^*)$	$d_{xy}(\pi^*)$	$d_{z^2}(\sigma^*)$
	−13.71 (H − 8)	−13.52 (H − 7)	−11.27 (H − 1)	−11.03 (H)	−5.11 (L)
$[Cu(H_2O)_4]^{2+}$					
square planar	d_{xz}	d_{yz}	$d_{z^2}(\sigma^*)$	$d_{xy}(\pi^*)$	$d_{x^2-y^2}(\sigma^*)$
	−12.77 (H − 6)	−12.76 (H − 5)	−12.13 (H − 4)	−11.77 (H − 2)	−5.02 (L)

[a]The most important (four occupied and one unoccupied) beta orbitals involved in the four d−d excited states are listed. The symbols H and L indicate HOMO and LUMO, respectively. The nature of the orbitals is defined as a d-type orbital when the Mulliken population of the d atomic orbital exceeds 90% and as a superposition of d atomic orbitals and the ligand orbitals when the Mulliken population is 10−90%. Notation such as $d_{xy}(\pi^*)$ means a π-type antibonding orbital consisting of the copper d_{xy} orbital and ligand lone pair orbitals.

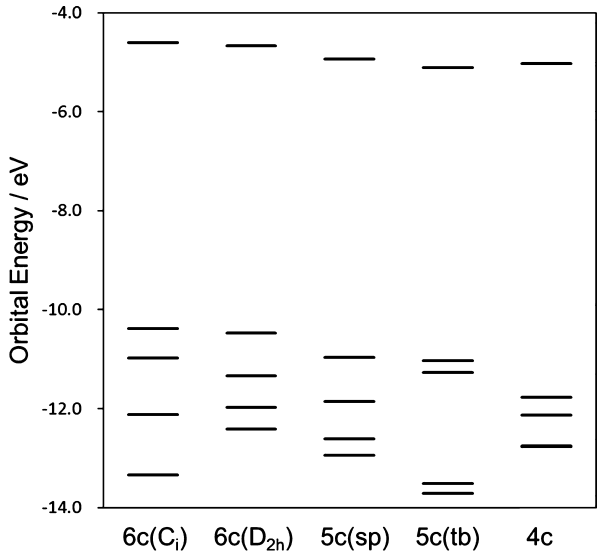

Figure 4. Energy levels of the d-type orbitals of $[Cu(H_2O)_{4-6}]^{2+}$. (6c(C_i): $[Cu(H_2O)_6]^{2+}$ square bipyramidal in the C_i symmetry, 6c(D_{2h}): $[Cu(H_2O)_6]^{2+}$ square bipyramidal in the D_{2h} symmetry; 5c(sp): $[Cu(H_2O)_5]^{2+}$ square pyramidal; 5c(tb): $[Cu(H_2O)_5]^{2+}$ trigonal bipyramidal; and 4c: $[Cu(H_2O)_4]^{2+}$ square planar).

The $[Cu(H_2O)_5]^{2+}$ (in square pyramidal and trigonal bipyramidal structures) + H_2O systems were very close in Helmholtz energy and were 11.1 and 11.2 kcal/mol higher than the lowest, respectively. The $[Cu(H_2O)_4]^{2+}$ + $2H_2O$ system was 17.7 kcal/mol higher than the lowest.

Table 1 also includes the Helmholtz energy (A) decomposition into the solute energy (E_{solute}), the excess chemical potential ($\Delta\mu$), eq 1, and the difference in E_{solute} and $\Delta\mu$ from the values of $[Cu(H_2O)_6]^{2+}$ in C_i symmetry (ΔE_{solute} and $\Delta\Delta\mu$). The difference ΔA between $[Cu(H_2O)_6]^{2+}$ in C_i and D_{2h} symmetries is mainly because of the solute energy E_{solute} (ΔE_{solute} is 8.20 kcal/mol and $\Delta\Delta\mu$ is −2.16 kcal/mol). The relative energy of $[Cu(H_2O)_4]^{2+}$, $[Cu(H_2O)_5]^{2+}$, and $[Cu(H_2O)_6]^{2+}$ is determined by the balance between the solute energy and the excess chemical potential. The relative solute energies ΔE_{solute} of the two $[Cu(H_2O)_5]^{2+}$ were larger than the two $[Cu(H_2O)_6]^{2+}$ by 21.7−32.4 kcal/mol, whereas the relative excess chemical potentials $\Delta\Delta\mu$ of the two $[Cu(H_2O)_5]^{2+}$ were smaller than the two $[Cu(H_2O)_6]^{2+}$ by 16.5−21.3 kcal/mol.

3.2. Molecular Structure and Solvation of a Six-Coordinate Complex $[Cu(H_2O)_6]^{2+}$. The six-coordinate structure is distorted from the octahedral geometries because of the John−Teller effect originating from the quasi-degenerate states of the complex, which show a sharp contrast to the nondegenerate ground-state complex like $[Cr(H_2O)_6]^{3+}$ in the previous paper.[13] $[Cu(H_2O)_6]^{2+}$ has near-octahedral (square bipyramidal) structures with two long axial (r_{ax}) and four short equatorial Cu−O bonds (r_{eq}). Two stable structures (in C_i and D_{2h} symmetries) were found in our calculations, as described in Section 3.1. The structural difference between the two structures is the orientation of the ligand water molecules, where in the C_i geometry, all ligand water molecules are perpendicular to each other, whereas in the D_{2h} geometry, four ligand water molecules point outward and are perpendicular to the equatorial plane of the complex.

The calculated geometrical parameters are shown in Figure 1. The Cu−O bond distances computed were r_{ax} = 2.28 Å and r_{eq} = 2.00/1.97 Å in the C_i symmetry and r_{ax} = 2.25 Å and r_{eq} = 2.04/1.96 Å in the D_{2h} symmetry. These values were in good agreement with the experimental values obtained from the EXAFS[2] in solution, that is, r_{ax} = 2.29−2.33 Å and r_{eq} = 1.95−2.01 Å, although the computed axial bond distances were slightly shorter. The values in vacuum computed by PBE0 were larger by about 0.01−0.05 Å. This can be attributed to the interaction between water ligands and solvent water molecules, which makes the complex ion more compact. Another factor was the electric polarization effect in water solution. The polarization from solution water molecules can disperse the electric charge and increase the attraction between the metal ion and ligands.

Figure 2a,b shows the SDFs of O for the structures in C_i and D_{2h} symmetries, respectively. In these illustrations, there are 12 high-distribution spots in the direction from O to H of the ligand water molecules. The distances of the solvent O with the highest-distribution spots from the H atoms of the ligands and the Cu atom are 1.51−1.99 and 3.70−3.91 Å, respectively. These data clearly show the hydrogen bonds between the

DOI: 10.1021/acs.jpca.9b01364
J. Phys. Chem. A 2019, 123, 3344−3354

Table 5. d−d Excitation Energies of $[Cu(H_2O)_{4-6}]^{2+}$ in Aqueous Solution (in eV)

structure	excitation energy	oscillator strength ($\times 10^5$)	excitation[a]	orbital picture	weight (%)[b]
$[Cu(H_2O)_6]^{2+}$					
square bipyramidal (C_i)					
	0.625	0	HOMO → LUMO	$d_{z^2}(\sigma^*) \rightarrow d_{x^2-y^2}(\sigma^*)$	90.9
	1.340	0	HOMO − 3 → LUMO	$d_{yz}(\pi^*) \rightarrow d_{x^2-y^2}(\sigma^*)$	60.2
			HOMO − 8 → LUMO	$d_{yz}(\pi) \rightarrow d_{x^2-y^2}(\sigma^*)$	39.2
	1.499	0	HOMO − 7 → LUMO	$d_{xz} \rightarrow d_{x^2-y^2}(\sigma^*)$	81.7
	1.590	0	HOMO − 9 → LUMO	$d_{xy}(\pi) \rightarrow d_{x^2-y^2}(\sigma^*)$	62.2
			HOMO − 4 → LUMO	$d_{xy}(\pi^*) \rightarrow d_{x^2-y^2}(\sigma^*)$	36.9
square bipyramidal (D_{2h})					
	0.660	0	HOMO → LUMO	$d_{z^2}(\sigma^*) \rightarrow d_{x^2-y^2}(\sigma^*)$	91.9
	1.378	0	HOMO − 4 → LUMO	$d_{xy}(\pi^*) \rightarrow d_{x^2-y^2}(\sigma^*)$	58.5
			HOMO − 10 → LUMO	$d_{xy}(\pi) \rightarrow d_{x^2-y^2}(\sigma^*)$	40.9
	1.536	0	HOMO − 8 → LUMO	$d_{xz} \rightarrow d_{x^2-y^2}(\sigma^*)$	81.8
	1.577	0	HOMO − 7 → LUMO	$d_{yz} \rightarrow d_{x^2-y^2}(\sigma^*)$	99.4
$[Cu(H_2O)_5]^{2+}$					
square pyramidal					
	0.941	4	HOMO → LUMO	$d_{z^2}(\sigma^*) \rightarrow d_{x^2-y^2}(\sigma^*)$	74.3
	1.440	27	HOMO − 6 → LUMO	$d_{xz}(\pi) \rightarrow d_{x^2-y^2}(\sigma^*)$	29.8
			HOMO − 1 → LUMO	$(d_{xz} + d_{yz})\ (\pi^*) \rightarrow d_{x^2-y^2}(\sigma^*)$	21.0
	1.551	13	HOMO − 7 → LUMO	$d_{yz}(\pi) \rightarrow d_{x^2-y^2}(\sigma^*)$	46.9
			HOMO − 2 → LUMO	$(d_{xz} - d_{yz})\ (\pi^*) \rightarrow d_{x^2-y^2}(\sigma^*)$r	23.3
	1.641	7	HOMO − 5 → LUMO	$d_{xy}(\pi^*) \rightarrow d_{x^2-y^2}(\sigma^*)$	35.4
			HOMO − 8 → LUMO	$d_{xy}(\pi) \rightarrow d_{x^2-y^2}(\sigma^*)$	30.5
			HOMO − 6 → LUMO	$d_{xz}(\pi) \rightarrow d_{x^2-y^2}(\sigma^*)$	22.0
trigonal bipyramidal					
	1.085	39	HOMO − 1 → LUMO	$d_{x^2-y^2}(\sigma^*) \rightarrow d_{z^2}(\sigma^*)$	82.9
	1.263	48	HOMO → LUMO	$d_{xy}(\pi^*) \rightarrow d_{z^2}(\sigma^*)$	46.6
			HOMO − 6 → LUMO	$d_{xy}(\pi) \rightarrow d_{z^2}(\sigma^*)$	43.9
	1.404	3	HOMO − 8 → LUMO	$d_{xz}(\pi) \rightarrow d_{z^2}(\sigma^*)$	41.0
			HOMO − 2 → LUMO	$d_{xz}(\pi^*) \rightarrow d_{z^2}(\sigma^*)$	31.8
			HOMO − 4 → LUMO	$d_{xz}(\pi^*) \rightarrow d_{z^2}(\sigma^*)$	23.2
	1.624	0	HOMO − 7 → LUMO	$d_{yz}(\pi) \rightarrow d_{z^2}(\sigma^*)$	70.5
			HOMO − 3 → LUMO	$d_{yz}(\pi^*) \rightarrow d_{z^2}(\sigma^*)$	27.2
$[Cu(H_2O)_4]^{2+}$					
square planar					
	1.598	1	HOMO − 2 → LUMO	$d_{xy}(\pi^*) \rightarrow d_{x^2-y^2}(\sigma^*)$	65.2
			HOMO − 7 → LUMO	$d_{yz}(\pi) \rightarrow d_{x^2-y^2}(\sigma^*)$	33.4
	1.665	2	HOMO − 4 → LUMO	$d_{z^2} \rightarrow d_{x^2-y^2}(\sigma^*)$	88.2
	1.977	5	HOMO − 5 → LUMO	$d_{yz} \rightarrow d_{x^2-y^2}(\sigma^*)$	53.6
			HOMO − 6 → LUMO	$d_{xz} \rightarrow d_{x^2-y^2}(\sigma^*)$	43.0
	1.988	2	HOMO − 6 → LUMO	$d_{xz} \rightarrow d_{x^2-y^2}(\sigma^*)$	54.0
			HOMO − 5 → LUMO	$d_{yz} \rightarrow d_{x^2-y^2}(\sigma^*)$	43.4

[a]The HOMO and LUMO in the table indicate the highest occupied beta molecular orbital and the lowest unoccupied beta molecular orbital, respectively. [b]The weights were calculated by $X^2 - Y^2$, where X and Y are the excitation and de-excitation amplitudes, respectively, in TD-DFT. Values larger than 20% are listed.

ligands and the solvent water molecules in the second hydration shell.

Figure 3a,c shows the RDFs of O and H from Cu obtained by angular averaging of the 3D distribution functions, as well as the CN of O. The RDFs for C_i and D_{2h} symmetries are very close to each other. In both graphs, the maxima of the RDFs are given at 4.4 and 5.0 Å for O and H, respectively [maximum values: 1.36 (O) and 1.28 (H)]. The graphs also show that there is no peak around 2 Å, as can be easily deduced from the SDFs. There are no additional water molecules in the first hydration shell except for the ligand water molecules, which is also confirmed from the oxygen CN graphs rising around 3.5 Å.

Figure 3b,d shows the RDFs of O and H from the O atom of the ligand water for the C_i and D_{2h} symmetries, respectively. Both RDFs have local maxima at about 2.9 and 3.5 Å for O and H, respectively [local maximum values: 1.08 (O) and 0.81 (H)]. These results indicate a typical solvation structure of a hydrogen bond between water molecules. This typical structure is common to the other structures of $[Cu(H_2O)_4]^{2+}$ and $[Cu(H_2O)_5]^{2+}$ in Figure 3f,h,j.

3.3. Molecular Structure and Solvation of the Five-Coordinate Complex $[Cu(H_2O)_5]^{2+}$. Pasquarello and co-workers examined the structure of the hydrated Cu^{2+} complex by both neutron diffraction and Car−Parrinello first-principles MD.[1] In contrast to the generally accepted picture, which assumes an octahedrally solvated Cu^{2+} ion, their experimental

DOI: 10.1021/acs.jpca.9b01364
J. Phys. Chem. A 2019, 123, 3344−3354

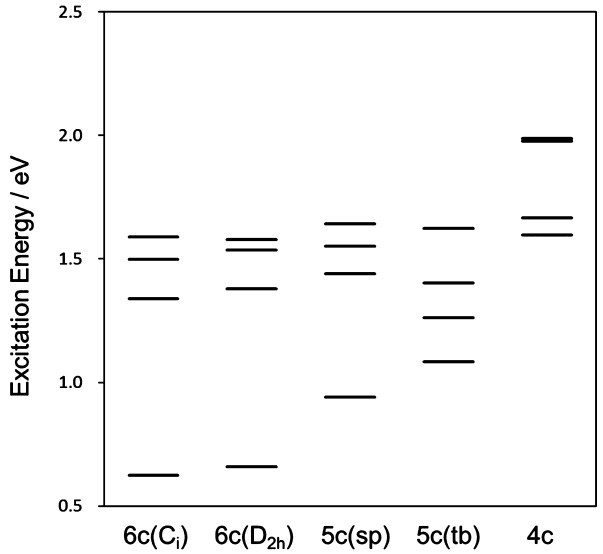

Figure 5. d−d Excitation energies of $[Cu(H_2O)_{4-6}]^{2+}$.

and theoretical results favored a fivefold coordination. Their simulation indicated that the solvated complex undergoes transformations between two $[Cu(H_2O)_5]^{2+}$ structures, namely, the square pyramidal and trigonal bipyramidal.

We found the square pyramidal and trigonal bipyramidal structures by the 3D-RISM-SCF optimization (Figure 1c,d). The Cu−O bond distances and the O−Cu−O angles are listed in Table 2. In Figure 1c, five O atoms in the ligand water molecules constitute a square pyramid and the Cu atom is located slightly inside the pyramid from the center of the bottom square. As in the $[Cu(H_2O)_6]^{2+}$ case, the H atoms of the ligand water molecules are all oriented outward the pyramid. The Cu−O bond distances for the bottom square are 1.95−1.98 Å, and the bond distance along the axis is 2.10 Å. The O−Cu−O angles are 92−100°. That is, its shape is a bit of a tall square pyramid with a slightly distorted square bottom. Another structure, the trigonal bipyramidal structure in Figure 1d, has a short axial bond distance of 1.93 Å and long equatorial bond distances of 2.06, 2.04, and 2.03 Å. Figure 3e shows the RDFs of O and H from Cu and the CN of O. The triangle is also slightly distorted from a regular triangle shape. The O−Cu−O angles are almost 90°; hence, the Cu atom is in the triangular plane.

Figure 2c shows the SDF of O for the square pyramidal structure. In the figure, the largest distribution spot and its distance from the Cu atom are specified. The largest distribution spot is located at 2.29 Å below the bottom plane of the pyramid (maximum value: 14.41). This result agrees well with the results of $[Cu(H_2O)_6]^{2+}$ in the D_{2h} symmetry. Figure 2d shows the SDF for the trigonal bipyramidal structure. The largest distribution spot of O is located outside the central triangle, opposite the most distant ligand water molecule. The distance from the Cu atom is 2.74 Å (maximum value: 7.25). We confirmed that there were no distributions located at similar positions, opposite the other two ligand water molecules in the triangle. In both structures, the distribution of O is at a position that supplements the five ligand water molecules and becomes part of a distorted octahedron.

Figure 3e,g shows the RDFs of O and H from the Cu atom and the CN of O for the square pyramidal and trigonal bipyramidal structures, respectively. Both graphs have very similar maximum peaks at the same positions as $[Cu(H_2O)_6]^{2+}$, although their maximum values are slightly smaller (1.33 (O) and 1.25 (H) for the square pyramidal and 1.32 (O) and 1.24 (H) for the trigonal bipyramidal structures). In addition to these maximum peaks, the RDF of O in Figure 3e has a small peak at 2.6 Å (local maximum value: 0.16), which means the distribution of water molecules in the first hydration shell. This clearly corresponds to the largest O distribution in the SDF (Figure 2c). Taking the CN at the local minimum (3.05 Å) between the first and second peaks of O RDF, the CN for the small RDF peak is given as about 0.4. In contrast, the RDF of O in Figure 3g has a shoulder at around 2.9 Å. The distribution corresponding to this shoulder is shown in Figure 2d. Taking the value at 3.05 Å, the CN of O is given at about 0.2. From these results, we can say that Cu^{2+} in $[Cu(H_2O)_5]^{2+}$ has 5.2−5.4 water molecules in the first hydration shell including the ligand water molecules.

3.4. Molecular Structure and Solvation of the Four-Coordinate Complex $[Cu(H_2O)_4]^{2+}$. Bérces and co-workers performed DFT and ab initio MD simulations to study the solvation of divalent copper by water.[22] They found that as the number of water molecules increases to above four, the additional ligands prefer to be hydrogen-bonded to the planar tetragonal primary hydration shell of $[Cu(H_2O)_4]^{2+}$ instead of filling the vacant axial position. Burda, Pavelka, and Šimánek performed a hydration study of Cu^{2+} cations in a variable water environment using the DFT method.[23] They concluded from stabilization energy calculations for the addition of water molecules that the Cu^{2+} cation prefers 4 (or 5) coordinate water molecules in the first solvation shell. These studies were based on cluster models, not being carried out in a solution environment. We examined the possibility of $[Cu(H_2O)_4]^{2+}$ in solution.

The optimized molecular structure is shown in Figure 1e and Table 3. We first carried out geometry optimizations from tetrahedron and planar structures. Both structures were finally converged to a nearly planar structure shown in the figure. The four O atoms constitute almost a square with the Cu atom at the center. The Cu−O bond distance was 1.95 Å. The water molecules were oriented outward of the square with their molecular plane perpendicular to the square. The Cu−O bond distances in vacuum were 1.954 and 1.956 Å; thus, the structure was very close to that in solution.

Figure 2e shows the SDF of O of solvent water molecules. In the figure, the two largest distribution spots are specified, which are located above and below the molecular plane and approximately at the vertices of the octahedron. The detailed distances between the largest distribution spot and the Cu atom were 1.95−1.96 Å. As in the $[Cu(H_2O)_5]^{2+}$ case, the ligand water and the O distribution spots constituted a distorted octahedron.

The RDF of O from the Cu atom in Figure 3i had a conspicuous peak at 2.2 Å (local maximum value: 0.74), which is in contrast to the small peak and the shoulder in $[Cu(H_2O)_5]^{2+}$. This peak clearly corresponds to the distributions of O in the SDF in Figure 2e. The CN of O around Cu was 1.3 at 3.1 Å, the local minimum of the RDF. This CN implies that Cu^{2+} has 5.3 water molecules in the first hydration shell including the ligand water molecules, which is very similar to the $[Cu(H_2O)_5]^{2+}$ case.

To summarize the results of $[Cu(H_2O)_{4-6}]^{2+}$, the Helmholtz energy calculations showed that the energy order was

DOI: 10.1021/acs.jpca.9b01364
J. Phys. Chem. A 2019, 123, 3344−3354

$A[6c(C_i)] < A[6c(D_{2h})] < A[5c(sp)] < A[5c(tb)] < A[4c]$. However, the five structures were close in Helmholtz energy, and the higher four structures were within 17.74 kcal/mol from the lowest one. In all the three structures of $[Cu(H_2O)_{4,5}]^{2+}$, the ligand water molecules and the largest O distribution spots constitute an octahedron like $[Cu(H_2O)_6]^{2+}$. The CNs were 5.2−5.4 for the two structures of $[Cu(H_2O)_5]^{2+}$ and 5.3 for the square planar structure of $[Cu(H_2O)_4]^{2+}$. These results provide us a picture for the Cu^{2+} in aqueous solution that several structures with 5−6 coordination water molecules were interchanged in the solution.

3.5. d−d Transitions of $[Cu(H2O)_{4-6}]^{2+}$ in Aqueous Solution. Cu^{2+} has the d^9 configuration, from which four d−d excited states arise in $[Cu(H_2O)_{4-6}]^{2+}$. Table 4 and Figure 5 show the d-type orbitals involved in the four excited states, and Table 5 shows the excitation energies and excitation patterns of the states.

In Table 4, only beta orbitals involved in the configurations with the largest weight in each state; hence, five d-type beta orbitals are listed. From a glance at Table 4 and Figure 4, the characters of the orbitals are easily understood from the analogy from the results of the crystal field theory, although the actual structures are distorted from the highly symmetric structures. The square pyramidal structures (C_i and D_{2h}) of $[Cu(H_2O)_6]^{2+}$ are deformations from the O_h structure with the d-orbital energy order $\varepsilon(d_{xy}) = \varepsilon(d_{xz}) = \varepsilon(d_{yz}) < \varepsilon(d_{z^2}) = \varepsilon(d_{x^2-y^2})$. The square pyramidal structure of $[Cu(H_2O)_5]^{2+}$ is a deformation from the C_{4v} structure with $\varepsilon(d_{xz}) = \varepsilon(d_{yz}) < \varepsilon(d_{xy}) < \varepsilon(d_{z^2}) < \varepsilon(d_{x^2-y^2})$. The trigonal bipyramidal structure is a deformation from the D_{3h} structure with $\varepsilon(d_{xz}) = \varepsilon(d_{yz}) < \varepsilon(d_{x^2-y^2}) < \varepsilon(d_{xy}) < \varepsilon(d_{z^2})$. The square planar structure is a deformation from the planar D_{4h} structure with $\varepsilon(d_{xz}) = \varepsilon(d_{yz}) < \varepsilon(d_{z^2}) < \varepsilon(d_{xy}) < \varepsilon(d_{x^2-y^2})$. Although the degeneracies are resolved by the distortions in the molecular structures, the orders of the orbital energies in Table 4 were consistent with these orders. In the six-coordinate complexes, the degeneracies were completely resolved, whereas in the five- and four-coordinate complexes, weak and strong quasi-degeneracies remained, respectively.

Other features can be seen in Table 4. One is that, as a whole, the orbital energy is more stable as the structure is stabilized and/or the CN is smaller. Another is that the stabilization is larger in the occupied orbitals than in the unoccupied orbitals, and hence, the gaps between the occupied and unoccupied orbitals increased. The gaps between occ4 and uoc1 in Table 4, for example, were 5.78, 5.80, 6.03, 5.92, and 6.72 eV, from the six-coordinate complex in the C_i symmetry through the four-coordinate complex.

The structures of the excitation energies in Table 5 and Figure 5 reflect the orbital levels mentioned above to some extent. The two structures of $[Cu(H_2O)_6]^{2+}$ have fairly low first excited states. The excitation energies were 0.625 and 0.660 eV for C_i and D_{2h} symmetries, respectively, because the ground and first excited states are originally degenerate if the structures have O_h symmetry. These first excited states are both characterized as d_{z^2} to $d_{x^2-y^2}$ excitation. The second to fourth states are triply degenerate in O_h symmetry, but they are well resolved. The excitation energies were in the range of 1.340−1.590 eV. These states consisted of the d_{xy}, d_{xz}, or d_{yz} to $d_{x^2-y^2}$ excitation. The excitation energies of the first excited states of $[Cu(H_2O)_5]^{2+}$ were 0.941 eV (d_{z^2} to $d_{x^2-y^2}$) and 1.085 eV ($d_{x^2-y^2}$ to d_{z^2}) for the square pyramidal and trigonal bipyramidal structures, respectively. The excitation energies of the second to fourth excited states were in the range of 1.263−1.641 eV. These states are mixtures of several single excitations with small weights. The maximum weights of each state were 29.8−70.5. As a result, the quasi-degeneracies of the d-type orbitals were not carried over to the excited states, and the energies of the states were well separated. Another feature of $[Cu(H_2O)_5]^{2+}$ is that the transitions have small oscillator strength (of the order of 10^{-4}) because the structures have no symmetry center. The square planar structure of $[Cu(H_2O)_4]^{2+}$ had high excited states compared with $[Cu(H_2O)_{5,6}]^{2+}$. The excitation energy of the first excited state was 1.598 eV (d_{xy} to $d_{x^2-y^2}$), which corresponds to the third or fourth excited state energies of the other complexes. In this structure, the third and fourth states were almost degenerate: 1.977 and 1.988 eV, which is a reflection of the quasi-degeneracy of the d_{xz} and d_{yz} orbitals.

The absorption spectra of aqueous solutions of Cu^{2+} showed a quite broad band, which clearly included several components: 1.17 eV (9400 cm^{-1}, $\varepsilon = 5$, $f = 1.0 \times 10^{-4}$) and 1.56 eV (12 600 cm^{-1}, $\varepsilon = 10$, $f = 2.6 \times 10^{-4}$).[24] Several calculated excitation energies in Table 5 agreed with the experimental value of 1.56 eV, and the first and second excited states of the trigonal bipyramidal structure of $[Cu(H_2O)_5]^{2+}$, 1.085 and 1.263 eV, respectively, were rather close to 1.17 eV. Some calculated transitions in Table 5 have little or no oscillator strength, but they should have some strength because of the structural fluctuation of the complexes in the solution. Considering the above-mentioned picture of the Cu^{2+} complex in solution (interchange of several structures), the experimental broad band in the spectra was interpreted as a superposition of excitation spectra of several structures of $[Cu(H_2O)_{4-6}]^{2+}$. We can probably say that the calculated results on the d−d excitations corresponded well to the experiment.

4. CONCLUSIONS

We investigated the molecular and solvation structures of the hydrated Cu^{2+} ion, $[Cu(H_2O)_6]^{2+}$, $[Cu(H_2O)_5]^{2+}$, and $[Cu(H_2O)_4]^{2+}$ and their excitation spectra using the 3D-RISM-SCF method.

We found five different geometrical structures: distorted octahedral $[Cu(H_2O)_6]^{2+}$ in C_i and D_{2h} symmetries, square pyramidal and trigonal bipyramidal $[Cu(H_2O)_5]^{2+}$, and square planar $[Cu(H_2O)_4]^{2+}$. For the six-coordinate complexes, we found two square bipyramidal structures in C_i and D_{2h} symmetries, both with two long axial bonds and four short equatorial bonds, and the bond lengths were in good agreement with the experimental data. The SDF showed 12 highest density spots of O, which were caused by the hydrogen bonds between the ligand and the solvent water molecules in the second hydration shell. For the five-coordinate complexes, we found a square pyramidal and a trigonal bipyramidal structure. From their SDFs, we could locate a position of the largest O distribution spot for each structure, which still constituted a distorted octahedron with five supplemental ligand water molecules. The RDFs obtained from the SDFs showed a small peak in the first hydration shell corresponding to the largest O distribution spot, and the CNs derived from RDFs indicated that the Cu^{2+} ion had 5.2−5.4 water ligands in the first hydration shell. For the four-coordinate complex, we found a square planar structure. The SDF gave us two spots of the largest O distribution, and they became parts of a distorted octahedron as well. The RDF and the associated CN indicated

DOI: 10.1021/acs.jpca.9b01364
J. Phys. Chem. A 2019, 123, 3344−3354

5.3 coordination water molecules in the first hydration shell of the Cu^{2+} ion. In separate studies of each coordinate complex, we showed that they had similar solvation structures from SDFs, RDFs, and CNs. These results indicated that the Cu^{2+} ion in an aqueous solution has 5−6 coordination water molecules in the first hydration shell, and structures with different CNs may be interchanged in the solution.

We calculated four low-lying excitations and electronic configurations using the TD-DFT method coupled with a 3D-RISM-generated electric field. The results gave us a similar picture to the classical crystal field theory because of the highly symmetrical features of all structures we studied. In the six-coordinate complexes, the degeneracies of excitation orbitals were resolved, whereas in the five- and four-coordinate complexes, weak and strong quasi-degeneracies remained. The excitation orbital energies were more stable when the CN decreased, and the gap between occupied and unoccupied orbitals decreased as well. Therefore, only the four-coordinate complex has generated the third and fourth excited states, whereas in other complexes, there was no obvious character of degeneracy. These results corresponded to the slight distortion of the structures from the symmetrical geometries. Comparing our calculation results with the absorption spectra, the d−d excitations also agreed well with the experiment.

Overall, our computational results give a consistent description on the molecular structure, solvation structure, and absorption spectra of Cu^{2+} complexes in aqueous solution, which can provide a new insight into the hydration of transition-metal ions.

■ ASSOCIATED CONTENT

Supporting Information

The Supporting Information is available free of charge on the ACS Publications website at DOI: 10.1021/acs.jpca.9b01364.

Assessments of the LJ parameter and the exchange−correlation functionals (PDF).

■ AUTHOR INFORMATION

Corresponding Authors

*E-mail: noriwo@chem.kyushu-univ.jp (N.Y.).
*E-mail: nakano@chem.kyushu-univ.jp (H.N.).

ORCID

Norio Yoshida: 0000-0002-2023-7254
Haruyuki Nakano: 0000-0002-7008-0312

Notes

The authors declare no competing financial interest.

■ ACKNOWLEDGMENTS

This work was supported by grants-in-aid [16H00842, 16K05519, and 18K05036] from MEXT, Japan. N.Y. also acknowledges the support of TOYOTA Riken Scholar from the Toyota Physical and Chemical Research Institute. Molecular graphics images were produced using the UCSF Chimera package.[25]

■ REFERENCES

(1) Pasquarello, A.; Petri, I.; Salmon, P. S.; Parisel, O.; Car, R.; Tóth, É.; Powell, D. H.; Fischer, H. E.; Helm, L.; Merbach, A. E. First Solvation Shell of the Cu(II) Aqua Ion: Evidence for Fivefold Coordination. *Science* **2001**, *291*, 856−859.

(2) Persson, I.; Persson, P.; Sandström, M.; Ullström, A.-S. Structure of Jahn−Teller Distorted Solvated Copper(II) Ions in Solution, and in Solids with Apparently Regular Octahedral Coordination Geometry. *J. Chem. Soc., Dalton Trans.* **2002**, *7*, 1256−1265.

(3) Schwenk, C. F.; Rode, B. M. New Insights into the Jahn−Teller Effect through Ab Initio Quantum-Mechanical/Molecular-Mechanical Molecular Dynamics Simulations of Cu(II) in Water. *ChemPhysChem* **2003**, *4*, 931−943.

(4) Schwenk, C. F.; Rode, B. M. Extended *Ab Initio* Quantum Mechanical/Molecular Mechanical Molecular Dynamics Simulations of Hydrated Cu^{2+}. *J. Chem. Phys.* **2003**, *119*, 9523−9531.

(5) Schwenk, C. F.; Rode, B. M. Influence of Electron Correlation Effects on the Solvation of Cu^{2+}. *J. Am. Chem. Soc.* **2004**, *126*, 12786−12787.

(6) Bryantsev, V. S.; Diallo, M. S.; van Duin, A. C. T.; Goddard, W. A., III Hydration of Copper(II): New Insights from Density Functional Theory and the COSMO Solvation Model. *J. Phys. Chem. A* **2008**, *112*, 9104−9112.

(7) Liu, X.; Lu, X.; Jan Meijer, E.; Wang, R. Hydration Mechanisms of Cu^{2+}: Tetra-, Penta- or Hexa-Coordinated? *Phys. Chem. Chem. Phys.* **2010**, *12*, 10801−10804.

(8) Rode, B. M.; Hofer, T. S.; Randolf, B. R.; Schwenk, C. F.; Xenides, D.; Vchirawongkwin, V. Ab Initio Quantum Mechanical Charge Field (QMCF) Molecular Dynamics: A QM/MM − MD Procedure for Accurate Simulations of Ions and Complexes. *Theor. Chem. Acc.* **2006**, *115*, 77−85.

(9) Moin, S. T.; Hofer, T. S.; Weiss, A. K. H.; Rode, B. M. Dynamics of Ligand Exchange Mechanism at Cu(II) in Water: An Ab Initio Quantum Mechanical Charge Field Molecular Dynamics Study with Extended Quantum Mechanical Region. *J. Chem. Phys.* **2013**, *139*, 014503.

(10) La Penna, G.; Minicozzi, V.; Morante, S.; Rossi, G. C.; Stellato, F. A First-Principle Calculation of the XANES Spectrum of Cu^{2+} in Water. *J. Chem. Phys.* **2015**, *143*, 124508.

(11) Kovalenko, A.; Hirata, F. Self-Consistent Description of a Metal−Water Interface by the Kohn−Sham Density Functional Theory and the Three-Dimensional Reference Interaction Site Model. *J. Chem. Phys.* **1999**, *110*, 10095−10112.

(12) Sato, H.; Kovalenko, A.; Hirata, F. Self-Consistent Field, Ab Initio Molecular Orbital and Three-Dimensional Reference Interaction Site Model Study for Solvation Effect on Carbon Monoxide in Aqueous Solution. *J. Chem. Phys.* **2000**, *112*, 9463−9468.

(13) Fujishige, S.; Kawashima, Y.; Yoshida, N.; Nakano, H. Three-Dimensional Reference Interaction Site Model Self-Consistent Field Study of the Electronic Structure of $[Cr(H_2O)_6]^{3+}$ in Aqueous Solution. *J. Phys. Chem. A* **2013**, *117*, 8314−8322.

(14) Kovalenko, A.; Hirata, F. Three-Dimensional Density Profiles of Water in Contact with a Solute of Arbitrary Shape: A RISM Approach. *Chem. Phys. Lett.* **1998**, *290*, 237−244.

(15) Perdew, J. P.; Ernzerhof, M.; Burke, K. Rationale for Mixing Exact Exchange with Density Functional Approximations. *J. Chem. Phys.* **1996**, *105*, 9982−9985.

(16) Adamo, C.; Barone, V. Toward Reliable Density Functional Methods without Adjustable Parameters: The PBE0 Model. *J. Chem. Phys.* **1999**, *110*, 6158−6170.

(17) Dunning, T. H. Gaussian Basis Sets for Use in Correlated Molecular Calculations. I. The Atoms Boron through Neon and Hydrogen. *J. Chem. Phys.* **1989**, *90*, 1007−1023.

(18) Balabanov, N. B.; Peterson, K. A. Systematically Convergent Basis Sets for Transition Metals. I. All-Electron Correlation Consistent Basis Sets for the 3d Elements Sc−Zn. *J. Chem. Phys.* **2005**, *123*, 064107.

(19) Berendsen, H. J. C.; Grigera, J. R.; Straatsma, T. P. The Missing Term in Effective Pair Potentials. *J. Phys. Chem.* **1987**, *91*, 6269−6271.

(20) Schmidt, M. W.; Baldridge, K. K.; Boatz, J. A.; Elbert, S. T.; Gordon, M. S.; Jensen, J. H.; Koseki, S.; Matsunaga, N.; Nguyen, K. A.; Su, S.; et al. General Atomic and Molecular Electronic Structure System. *J. Comput. Chem.* **1993**, *14*, 1347−1363.

DOI: 10.1021/acs.jpca.9b01364
J. Phys. Chem. A 2019, 123, 3344−3354

(21) Yoshida, N.; Hirata, F. A New Method to Determine Electrostatic Potential around a Macromolecule in Solution from Molecular Wave Functions. *J. Comput. Chem.* **2006**, *27*, 453−462.
(22) Bérces, A.; Nukada, T.; Margl, P.; Ziegler, T. Solvation of Cu^{2+} in Water and Ammonia. Insight from Static and Dynamical Density Functional Theory. *J. Phys. Chem. A* **1999**, *103*, 9693−9701.
(23) Burda, J. V.; Pavelka, M.; Šimánek, M. Theoretical Model of Copper Cu(I)/Cu(II) Hydration. DFT and Ab Initio Quantum Chemical Study. *J. Mol. Struct.: THEOCHEM* **2004**, *683*, 183−193.
(24) Sutton, D. *Electronic Spectra of Transition Metal Complexes: An Introductory Text*; MacGraw-Hill European Chemistry Series; McGraw-Hill, 1968.
(25) Pettersen, E. F.; Goddard, T. D.; Huang, C. C.; Couch, G. S.; Greenblatt, D. M.; Meng, E. C.; Ferrin, T. E. UCSF Chimera—A Visualization System for Exploratory Research and Analysis. *J. Comput. Chem.* **2004**, *25*, 1605−1612.

DOI: 10.1021/acs.jpca.9b01364
J. Phys. Chem. A 2019, 123, 3344−3354